

NURBS

* * ** ***

NURBS Interpolator for Controlling the Surface Roughness

Inhugh Choi*, Taesung Jung*, Wonpyo Hong** and Minyang Yang***

Key Words : NURBS interpolator (NURBS), PC-NC (PC), Variable feedrate (), Extended surface roughness model ()

Abstract

Finish machining of a curved surface is often carried out by an NC system with curve interpolation in the field. This NURBS interpolation adopts a feedrate optimizing strategy based on both the geometrical information and dynamic properties. In case of a finish cut using a ball-end mill, the curve interpolator needs to take the machining process into account for more improved surface, while reducing the polishing time. In this study, the effect of low machinability at the bottom of a tool on surface roughness is also considered. A particular curve interpolation algorithm is proposed for generating feedrate commands which are able to control the roughness of a curved surface. The simulation of the machined surface by the proposed algorithm was carried out, and experimental results are presented.

1. CNC , Yang(1-3)
가 CNC 가
가 , Taylor
()
(contour error) (feedrate error)
Lo⁽⁴⁾ , Yeh⁽⁵⁾
CNC
(direct interpolation)
, Lo⁽⁷⁾ CC (cutter contact)
, Chu⁽⁸⁾ 가 가
(local shape)
, Farouki⁽⁹⁾

*
E-mail : s_cih2000@kaist.ac.kr
TEL : (042)869-3264 FAX : (042)869-3210
**
가

PH (Pythagorean-hodograph)
MRR (material removal rate)
CNC

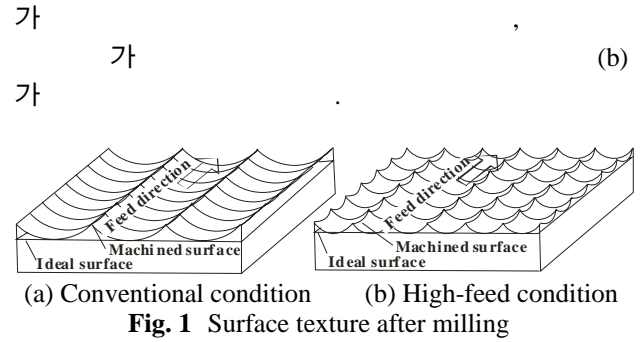
MRR 가
가 가 MRR 가
가 가 MRR 가
가 가 MRR 가

가 가
(10) 가
(path interval) (cusp) 가
(cutter mark)
가 가
(11-14)

가
NURBS Z-map 가
가 NURBS
remains) 가
(13)
5 가
, 3 가 가

2. 가

가 가
(topology) 가
가
가 Fig.1



2.1

가
(1)

$$R_{max} = \frac{f_f^2}{8r} \left(1 - \frac{r}{\rho_f + r}\right) + \frac{f_p^2}{8r} \left(1 - \frac{r}{\rho_p + r}\right) \quad (1)$$

, f_t , f_p
r 가
가 가 가 가 가
가 가 가
(11)
(12)
(13)
(14)
(15)
(16)
(17)
(18)
(19)
(20)
(21)
(22)
(23)
(24)
(25)
(26)
(27)
(28)
(29)
(30)
(31)
(32)
(33)
(34)
(35)
(36)
(37)
(38)
(39)
(40)
(41)
(42)
(43)
(44)
(45)
(46)
(47)
(48)
(49)
(50)

2.2

가 Fig.2

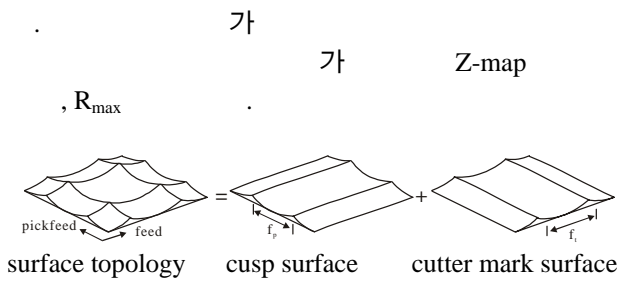
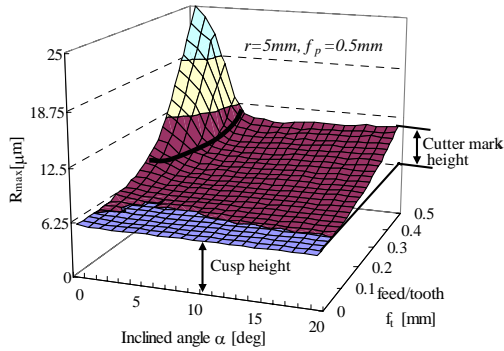
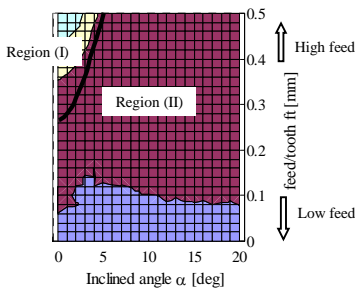


Fig. 2 Surface topology by the superposition of the component surfaces in the two directions



(a) Map of R_{max}



(b) Contour map of R_{max}

Fig. 3 Resultant surface roughness from the simulation

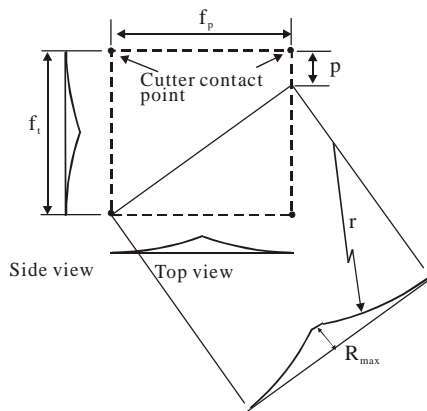


Fig. 4 Feature drawing of machined surface in the non-effect zone of dead center

Fig.3 5mm, 0.5mm/tooth

R_{max} , (I)
 R_{max} 가 2
 가, (II)
 가
 가
 가
 가

Fig.4
 (II) R_{max} 가
 R_{max}
 가 (2)

$$R_{max}(f_t, |\alpha| > \alpha_c) = \frac{f_p^2}{8r} \cdot \left[1 + \left(\frac{f_t - p}{f_p} \right)^2 \right] \quad (2)$$

$$p = \frac{f_t}{\pi} \cdot \frac{f_p}{r \sin \alpha} \cdot f_t$$

가 . 가

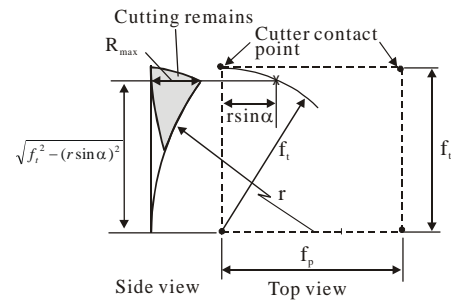


Fig. 5 Feature drawing of machined surface in the effect zone of dead center

Fig.5
 (I) R_{max} 가

가
 $r \sin \alpha$
 가

$$R_{max}(f_t, |\alpha| \leq \alpha_c) = r \cdot \left[1 - \sqrt{1 - \left(\frac{f_t}{r} \right)^2 + \sin^2 \alpha} \right] \quad (3)$$

(3)

R_{max}
가

, f_i 0.53 f_p f_p
가 .
0.27mm/tooth 0.5mm/tooth 가

(4)

α_c

$$\alpha_c = \sin^{-1} \left(\frac{1}{r} \sqrt{\left(\frac{A}{8r}\right)^2 - \frac{A}{4} + f_i^2} \right) \quad (4)$$

$$, A = f_p^2 + (f_i - p)^2 , p = \frac{f_p}{2\pi}$$

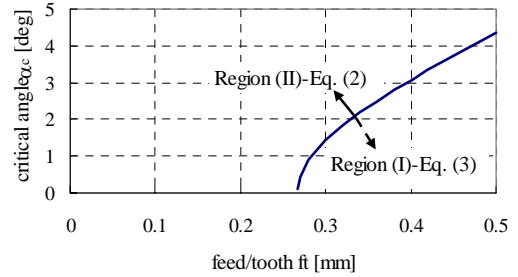
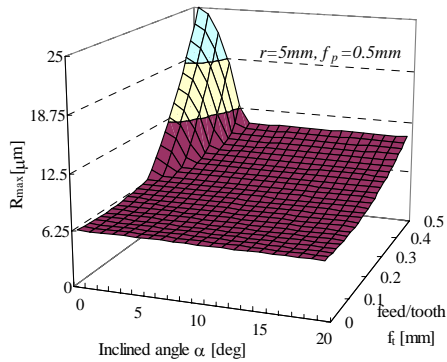
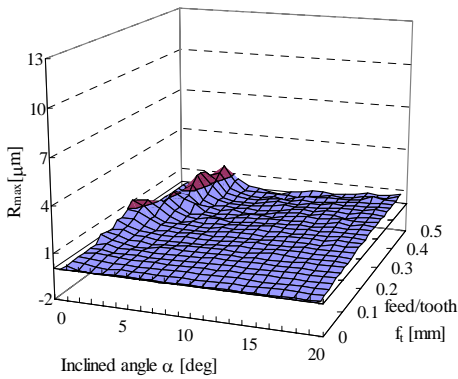


Fig. 7 Critical inclination angle according to feed per tooth



(a) Extended surface roughness model



(b) Error map from simulated surface
(max. error = 1.8um)

Fig. 6 Extended surface roughness of the surface machined by ball-end mill

, 가 R_{max} (2)
(3)
가 . Fig.6

Fig.3

1.8um

Fig.7

R_{max}

4

3.

NURBS

3.1

, CAM

가

, 가 가

. 2

2 가
가

(5) (6)

$$f_i = \frac{f_p}{2\pi} + \sqrt{8r \cdot R_{max} - f_p^2} \quad |\alpha| > \alpha_c \quad (5)$$

$$f_i = \sqrt{(r \sin \alpha)^2 + 2r \cdot R_{max} - R_{max}^2} \quad |\alpha| \leq \alpha_c \quad (6)$$

가

$2\alpha_c$

가

(isotropic surface)

가

Fig.8

가

/

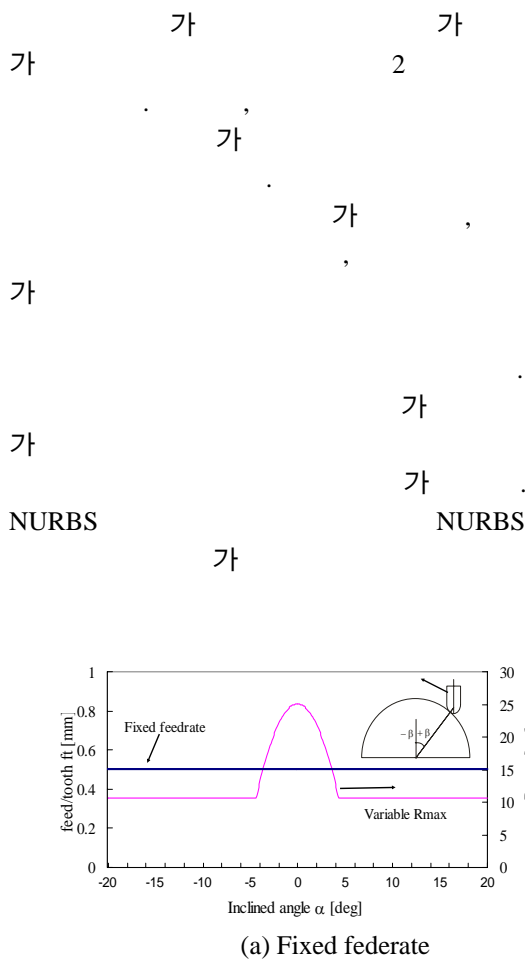


Fig. 8 Relationship between the feed per tooth and the roughness

3.2 NURBS

$$P(u) = [x(u) \quad y(u) \quad z(u)]$$

$$\left(\Delta s_d \right) \quad FT/60(\mu m)$$

$$F$$

$$(mm/min) \quad , \quad T$$

$$(msec)$$

$$(\Delta u)$$

Taylor (7)

$$u_{i+1} = u_i + \frac{\Delta s_d}{|\dot{P}(u)|} - \frac{\Delta s_d^2 \left(\dot{P}(u) \cdot \ddot{P}(u) \right)}{2|\dot{P}(u)|^4} \quad (7)$$

$$\dot{P}(u) = \frac{dP(u)}{du} \quad , \quad \ddot{P}(u) = \frac{d^2 P(u)}{du^2}$$

$$f_t \quad 2Sf_i T / 60 (\mu m) \quad (5) \quad (6)$$

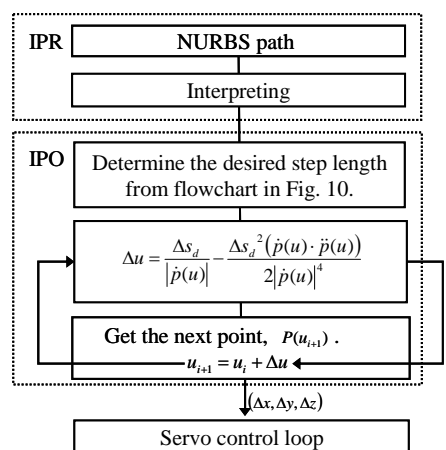


Fig. 9 Layout of the proposed curve interpolator

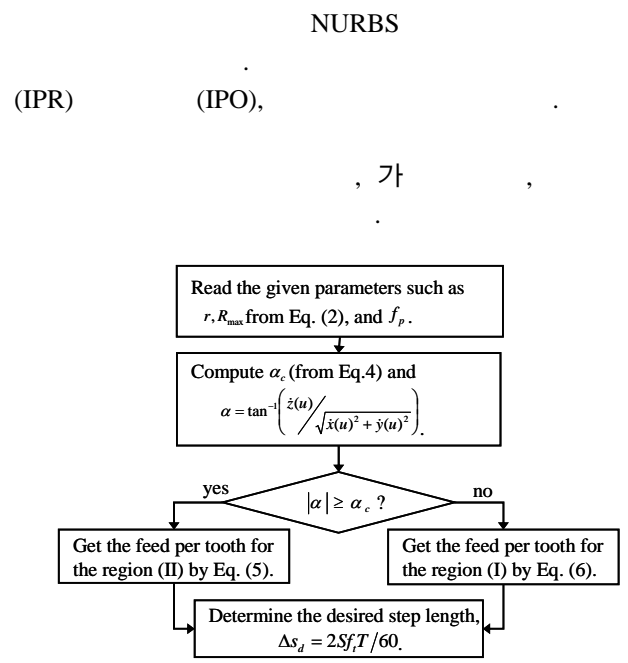


Fig. 10 Flowchart for getting a set of step length based on the target roughness

Fig.10

2.

3. (5) (6)

4. (7) NURBS

5

4. 가

4.1

PC-NC
NT
RTX (VentureCom Co.)
4msec

가 가
5mm, 0.5mm/tooth,
Al2024

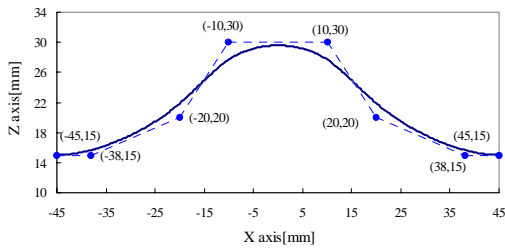


Fig. 11 An example of NURBS tool path designed for upward and downward milling (knot vector [0 0 0 0 0.2 0.4 0.6 0.8 1 1 1 1])

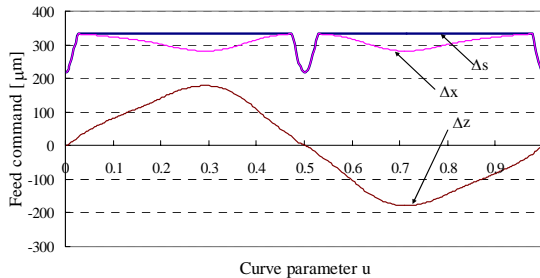


Fig. 12 Feed command controlled by proposed algorithm on a NURBS tool path

3 NURBS
NURBS

Fig.12

0.5
가
4.3°
65%

가

4.2

Z-map 가 가

10° 가

Fig.13

Fig.13(a) 가 Z-map

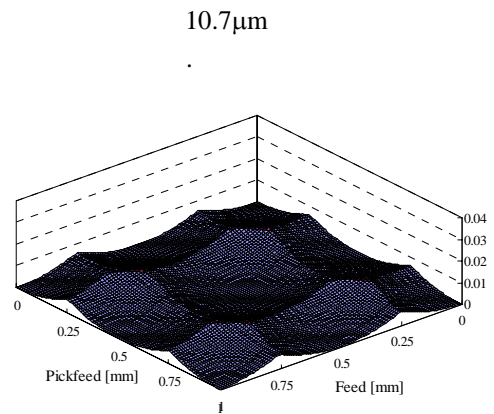
10.7μm

(2)

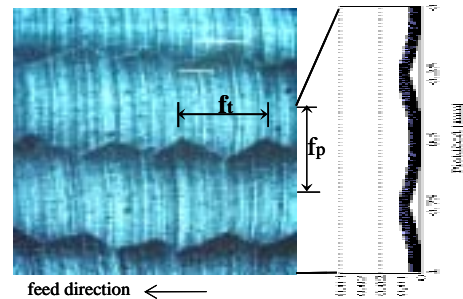
가

R_{max}

(2)



(a) Simulated surface ($R_{max}=10.7\mu m$)



(b) Actual machined surface

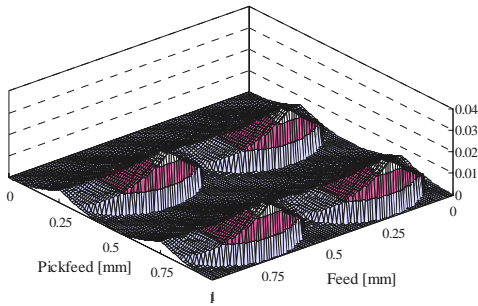
Fig. 13 Machined surface when $\alpha=10^\circ$ and $f_t/f_p=1$

Fig.14

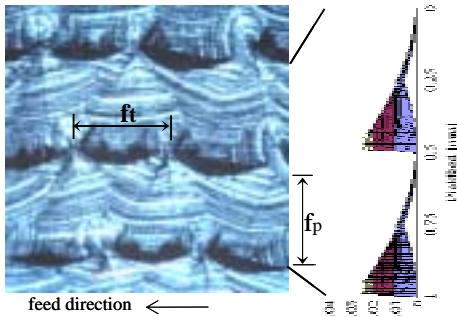
0°

가 가
 가 , 가 2
 가 가 Z-map
 가 가
 가 가

(rubbing)



(a) Simulated surface ($R_{max}=24.9\mu m$)



(b) Actual machined surface

Fig. 14 Surface by the fixed feedrate when $\alpha=0^\circ$ and $f_v/f_p=1$

가 (6)

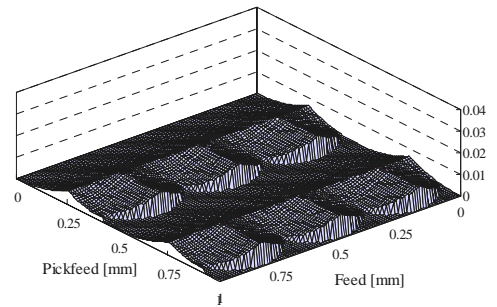
가 가 Fig.15
 0° R_{max} 10.2 μm
 가 가 0.33mm
 가

가 가 가
 가 가

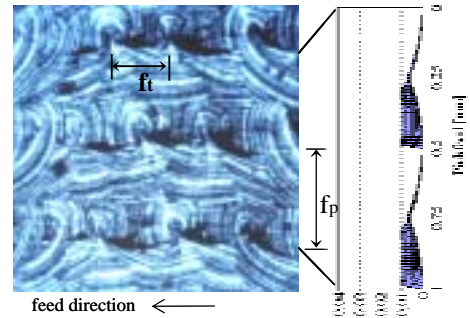
Fig.16 가 (Marsurf, Mahr)
 가 R_{max}

17.4 μm 9.3 μm

2 μm



(a) Simulated surface ($R_{max}=10.2\mu m$)



(b) Actual machined surface

Fig. 15 Surface controlled by the variable feedrate when $\alpha=0^\circ$ and $f_v/f_p=0.65$

5.

NURBS
 가

PC-NC NURBS

가

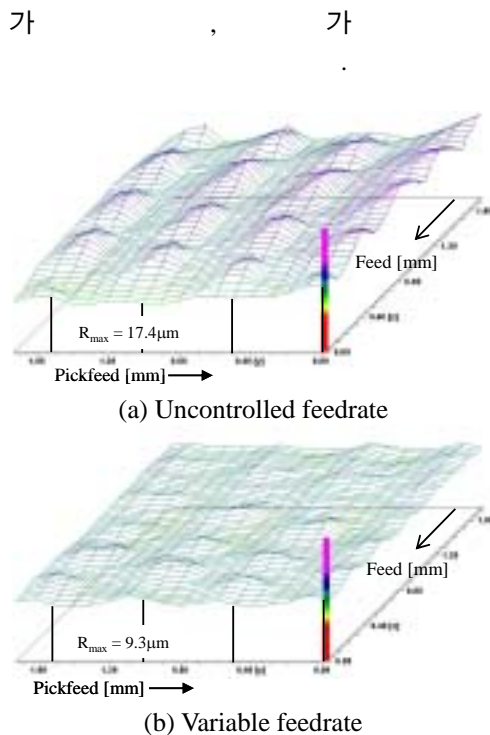


Fig. 16 Surface topology measured when $\alpha=0^\circ$

- (1) J. J. Chou and D. C. H. Yang, 1991, "Command generation for three axis CNC machining," *Journal of Engineering for Industry, Trans. of the ASME*, Vol. 113, pp. 305-310.
- (2) J. J. Chou and D. C. H. Yang, 1992, "On the generation of coordinated motion of five-axis CNC/CMM machine," *Journal of Engineering for Industry, Trans. of the ASME*, Vol. 114, pp. 15-22.
- (3) D. C. H. Yang and J. J. Chou, 1994, "Automatic generation of piecewise constant speed motion with smooth transition for multi-axis machines," *Journal of Mechanical Design, Trans. of the ASME*, Vol. 116, pp. 581-586.
- (4) C. C. Lo, 1997, "Feedback interpolators for CNC machine tools," *Journal of Manufacturing Science and Engineering, Trans. of the ASME*, Vol. 119, pp. 587-592.
- (5) S. S. Yeh and P. L. Hsu, 1999, "The speed-controlled interpolator for machining parametric curves," *Computer-Aided Design*, Vol. 31, pp. 349-357.
- (6) S. S. Yeh and P. L. Hsu, 2002, "Adaptive-feedrate interpolation for parameteric curves with a confined chord error," *Computer-Aided Design*, Vol. 34, pp. 229-237.
- (7) C. C. Lo, 1998, "A new approach to CNC tool path generation," *Computer-Aided Design*, Vol. 30, No.8, pp. 649-655.
- (8) C. N. Chu, S. Y. Kim, B. H. Kim and J. M. Lee, 1997, "Feedrate optimization of ball end milling considering local shape features," *Annals of CIRP*, Vol. 46, pp. 433-436.
- (9) R. T. Farouki, J. Manjunathaiah, D. Nicholas, G. F. Yuan and S. C. Jee, 1998, "Variable-feedrate CNC interpolators for constant material removal rates along pythagorean-hodograph curves," *Computer-Aided Design*, Vol. 30, No. 8, pp. 631-640.
- (10) R. Baptista and J. F. Antune, 2000, "Three and five axes milling of sculptured surface," *Journal of Materials Processing Technology*, 103, pp. 398-403.
- (11) R. S. Lin and Y. Koren, 1996, "Efficient tool-path planning for machining free-form surface," *Journal of Engineering for Industry, Trans. of the ASME*, Vol. 118, pp. 20-28.
- (12) B. H. Kim and C. N. Chu, 1994, "Effect of cutter mark on surface roughness and scallop height in sculptured surface machining," *Computer-Aided Design*, Vol. 26, No. 3, pp. 179-188.
- (13) N. Koreta, T. Egawa, M. Kuroda, K. Watanabe and Y. Li, 1993, "Analysis of surface roughness generation by ball endmill machining," *Japan Society for Precision and Engineering*, Vol. 59, No. 9, pp. 129-134(in Japan).
- (14) K. Naito, K. Ogo, T. Konaga, T. Abe, K. Kanda and M. Matsuoka, 1994, "Development of ball end milling for fine high-efficiency finishing," *International Journal of Japan Society for Precision and Engineering*, Vol. 28, No.2, pp. 105-110.